

Ocean processes and seasonal inflow along Ronne Ice Front

Keith Makinson

*British Antarctic Survey, Natural Environment Research Council,
High Cross, Madingley Road, Cambridge, CB3 0ET, U.K.*

Michael Schröder

*Alfred-Wegener Institute for Polar and Marine Research,
Bussestraße 24, 27570 Bremerhaven, Germany*

Introduction

Throughout much of the year a coastal polynya along Ronne Ice Front is maintained by tidal action and offshore winds [Renfrew *et al.*, 2002]. During summer months this polynya enlarges as solar radiation warms the surface waters, while in wintertime, the polynya exposes the relatively warm water to the cold atmosphere causing the seawater to cool to its surface freezing point. Further heat loss results in the formation of sea ice and salinification of the seawater, converting it into High Salinity Shelf Water (HSSW) throughout the entire water column. This cold dense water mass has been observed to flow along and towards the ice front [Foldvik *et al.*, 2001; Nicholls *et al.*, 2003] and drain deep into the sub-ice shelf cavity [Nicholls and Makinson, 1998]. Through interactions with the base of Filchner-Ronne Ice Shelf (FRIS), the HSSW is converted to Ice Shelf Water (ISW), a water mass that is fresher, and by definition, colder than the surface freezing point. Ultimately this water reaches the northerly point of Filchner Depression where it overflows the continental shelf break [Nicholls *et al.*, 2001].

Along Ronne Ice Front however, dynamical arguments suggest that the step change in water column thickness poses a considerable barrier to flow across it. Some numerical simulations further highlight this effect [Gerdes *et al.*, 1999] while others suggested a seasonal flow into the cavity [Jenkins *et al.*, Submitted] that is consistent with sub-ice shelf observations [Nicholls and Makinson, 1998]. Using instrumented moorings along Ronne Ice Front, two areas of HSSW inflow have been identified, one in the central ice front just west of Berkner Bank [Foldvik *et al.*, 2001] and the second in Ronne Depression [Nicholls *et al.*, 2003]. However, little is known about the mechanisms that control the inflows beneath the ice shelf. Using data from mooring FR6 located in the western part of Ronne Depression just north of the ice front, the aim of this work is to identify ice front processes that may control the flow of HSSW into the sub-ice shelf cavity.

Mooring data

Mooring FR6 was located 5-10 km from the ice front for a period of over two years and was deployed in February 1995. The water depth was 613 m and instruments were located at depths of 261 m, 442 m and 588 m, and the nearby ice shelf draft was approximately 220 m. In addition to current meters at those depths some temperature and salinity data were also obtained.

The current meter data are dominated by semi-diurnal tides with velocities up to 30 cm s⁻¹ with other mean flows superimposed. To remove the tidal currents, a harmonic analysis was performed to reveal the residual currents. These currents were partitioned into frequency ranges of 0-1 day, 1-10 days and +10 days using high, band and low pass filters. Within each of the partitions the signal amplitude varies on a seasonal time scale. During late summer and early winter there are significant currents close to semi-diurnal frequencies followed by considerable wintertime

activity in the 1-10 day band. In the longer-term mean flow there is a southerly component towards the ice shelf cavity that is strongest during late summer. Within the rest of Ronne Depression there is a strong east to west flow along the ice front and once HSSW production ceases, ISW exits the ice shelf cavity on the eastern side of Ronne Depression and is advected along the ice front before re-entering the cavity around FR6 [Nicholls *et al.*, 2003]. This pattern of circulation leads to a cooling and freshening of the mid-water column at FR6 during late summer and early winter.

Tidal processes

In order to reveal the seasonal signal in the tidal record, a harmonic tidal analysis was applied to short sections of data. The analysis was applied to the initial 662-hour section of current meter data to separate six tidal constituents (Q_1 , O_1 , K_1 , N_2 , M_2 , and S_2) and then repeated by moving the 662-hour window forward in steps of 24 hours until the end of the record was reached. The tidal current contribution for each constituent can be represented as a vector whose tip traces out an ellipse of the period of the constituent. Four parameters, the amplitude (R_+ and R_-) and phase (φ_+ and φ_-) of two co-rotating vectors (Figure 1), can be used to characterize a tidal ellipse.

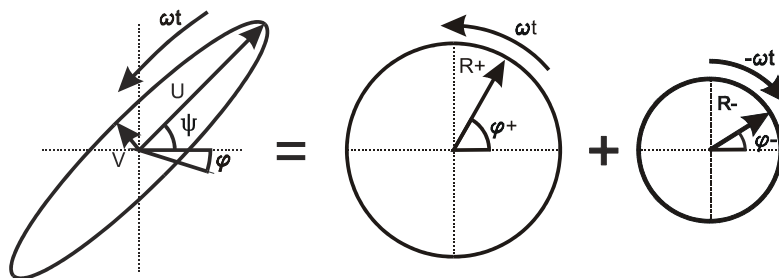


Figure 1. The basic parameters of a tidal ellipse and its two counter rotating components.

The time series of R_+ and R_- for M_2 at 442 m is shown in Figure 2 together with R_+ for S_2 and N_2 , highlighting the seasonality of the semi-diurnal tides. Figure 3 also shows the M_2 velocity profile for R_+ and R_- in both winter and summer. The seasonal vertical structure of the tidal current is almost identical to tidal current profiles that resulted from modelling the stratified and non-stratified water column beneath FRIS [Makinson, 2002]. The model demonstrated how semi-diurnal R_+ profiles had large boundary layers that could be dramatically modified by changes in stratification, while R_- with small boundary layers was unaffected. These large R_+ boundary layers result from, and increase in depth with, proximity to the critical latitude, where the inertial or Coriolis frequency equals the tidal frequency. At FR6 the M_2 critical latitude lies only 26 km to the north at $74^{\circ}28'18''S$.

The amplitude of R_+ (M_2) exhibits a two-fold increase signifying the developing stratification at FR6 during summer months (Figure 2 and 3). Also, despite the remoteness of the other semi-diurnal critical latitudes, the amplitudes of R_+ (S_2) and R_+ (N_2) show a significant increase as a result of changes in stratification. It should be noted that in this analysis, K_2 is not separated from S_2 and there is an underlying six month signal with an amplitude of 0.013 m s^{-1} remaining even in R_- (S_2). Nevertheless, a signal associated with summer stratification is visible within R_+ (S_2). Therefore, the semi-diurnal tides, and the M_2 R_+ tidal current profile in particular, can act as a proxy measure of summer stratification.

The profile of the two M_2 rotary tidal current components (Figure 3) show that, during wintertime, the R_+ boundary layer occupies around 200 m of the lower water column because of

the nearby critical latitude, with R_+ having an almost uniform profile. However, through the summer, and despite FR6 being offshore, the lower two thirds of the R_+ profile matches the modelled current profiles found beneath the ice shelf. Clearly, during periods of stratification (Figure 4a and b) the presence of the ice shelf base influences currents several kilometres offshore, with the amplitude of R_+ decreasing in the mid-water column (442 m to 261 m) because of friction from the ice shelf base, while R_+ remains unaffected (Figure 3). This suggests that the portion of the water column below the draft of the ice shelf is decoupled from the upper water column, creating an enhanced tidal flow in and out of the ice shelf cavity that extends several

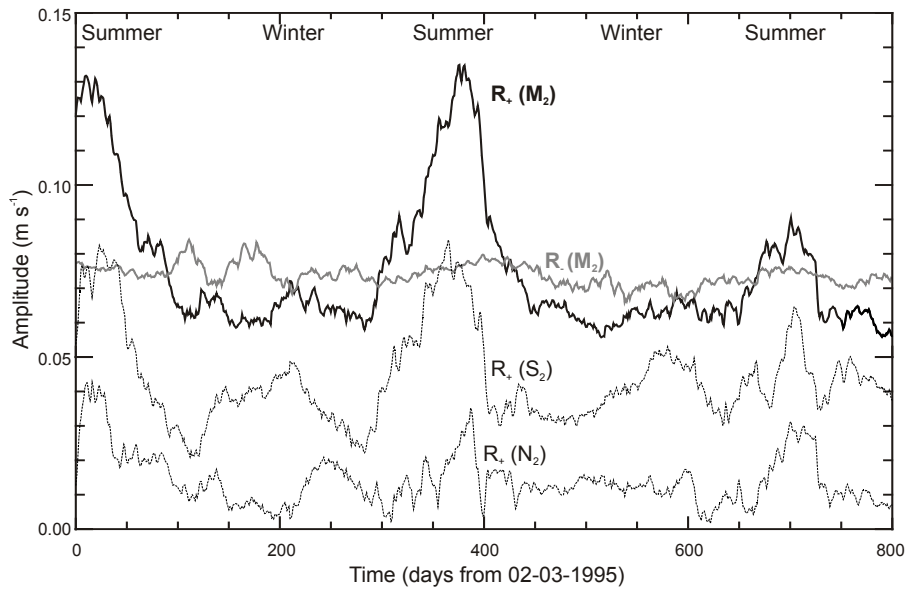


Figure 2. The seasonal variability of the clockwise and anticlockwise rotary tidal current components for M_2 at mooring FR6 at a depth of 442 m. The anticlockwise component of S_2 and N_2 are indicated by the dotted lines.

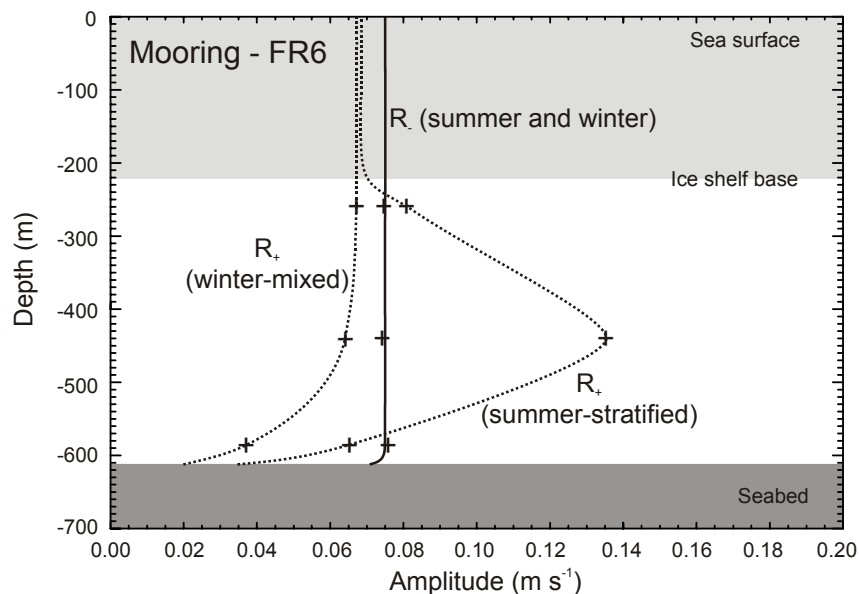


Figure 3. The clockwise and anticlockwise tidal current components for M_2 at mooring FR6. The portion of water column occupied by the nearby ice shelf is indicated by the light shading and the seabed is indicated with the darkest shading. The crosses are current meter measurements and the lines indicate the extrapolated vertical current profiles for a well mixed and stratified water column with R_+ remaining unaffected.

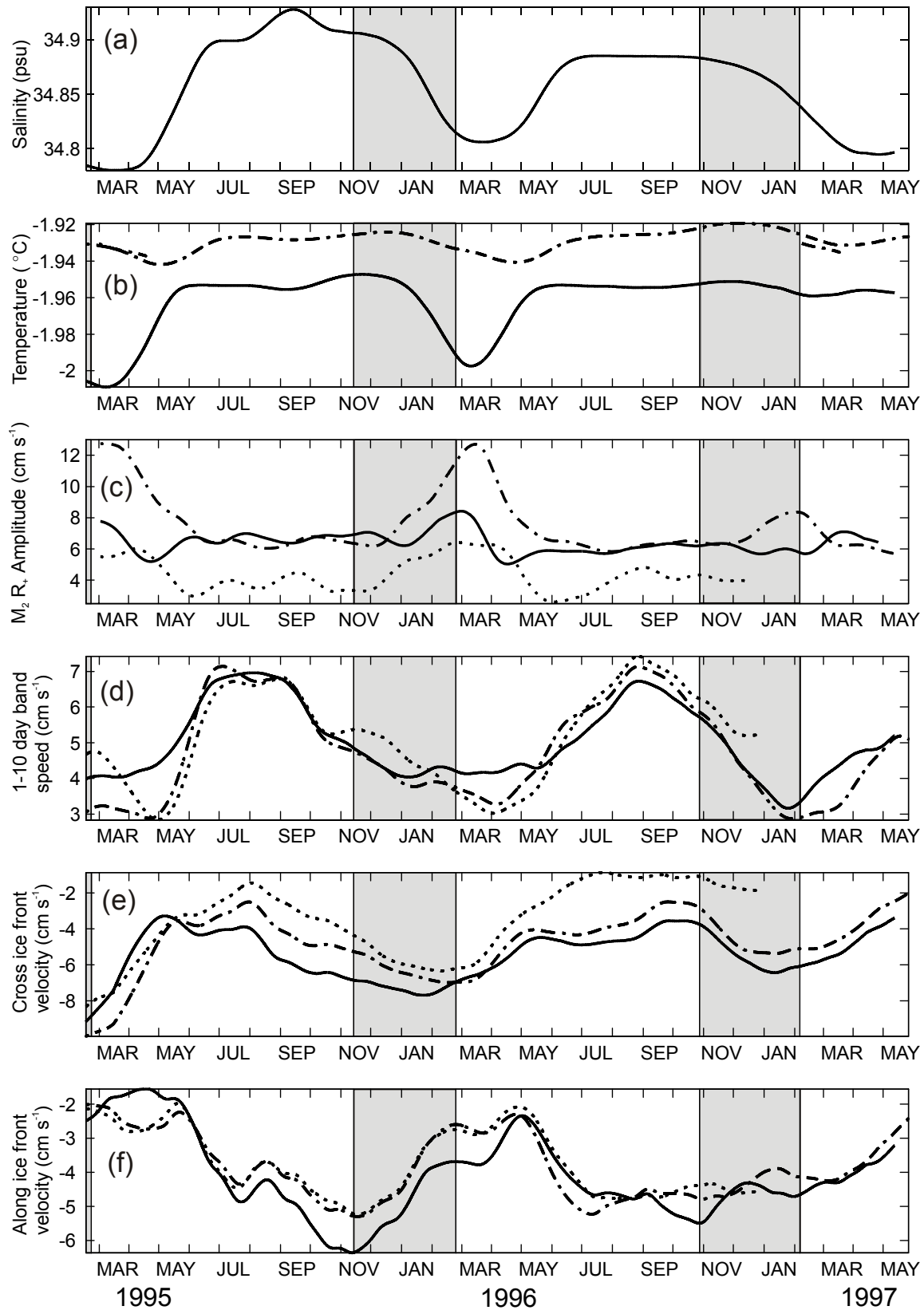


Figure 4. Low pass filtered time series from FR6 mooring instruments at 261 m (solid lines), 442 m (dashed lines) and 588 m (dotted lines). The shaded areas show the summer melting season from *Renfrew et al* [2002].

kilometers offshore. This tidal flow feature shows that any dynamical constraints no longer impede the passage of water across the ice front into the sub-ice shelf cavity, and, consequently, that the maximum inflow coincides with the enhanced $M_2 R_+$ currents (Figure 4c and e). Also, with the development of the two large turbulent boundary layers (Figure 3), it is presently unclear if they aid or maintain the decoupling from the upper water column.

In addition, a further contribution to the inflow at FR6 could result from tidally driven mean currents. However, previous modelling studies have shown that around FR6 tidally driven mean flows are very small and no inflows are indicated [Makinson and Nicholls, 1999].

Winter sea ice and eddy formation

During the winter freezing season (March-October) there is intense sea ice production and formation of HSSW in the coastal polynya along Ronne Ice Front. During this period the currents in the 1-10 day band increase (Figure 4d), peaking in the late winter and decaying once sea ice formation decreases and the freezing season ends. Inspection of the mooring data shows coherent structures extending throughout the water column with horizontal extents of 10-15 km and velocities of up to 10-20 cm s^{-1} (Figure 5). These features are likely to be generated by instabilities in the front between dense HSSW and lighter adjacent water masses resulting in meanders and eddies that are consistent with studies of dense water production in coastal polynyas [Chapman, 1999].

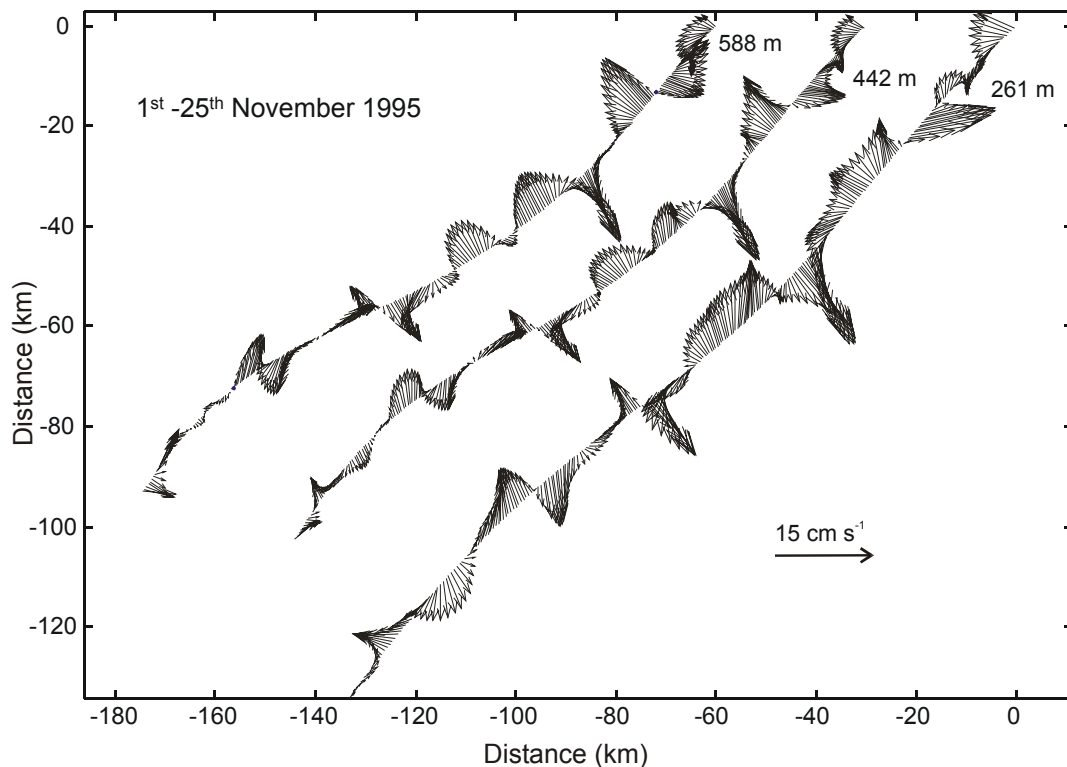


Figure 5. Mooring FR6 vector plots for currents in the 1-10 day band superimposed on progressive mean flow plot.

Through this winter period the along ice front velocity increases (Figure 4f) possibly due to the density contrast of water masses either side of the ice front driving the flow along the front. However during this period the inflow decreases rapidly (Figure 4e), soon after the onset of freezing, as the water column becomes fully mixed and eddy type structures form. This

diminished inflow is consistent with the dynamical arguments that require the water column to follow lines of constant water column thickness rather than cross the topographic step at the ice front.

Summary

At this inflow site, the FR6 mooring data suggest that stratification in the water column is a contributing factor governing the rate of inflow of HSSW into the sub-ice shelf cavity. During the latter half of the winter, the intense production of HSSW forms and maintains a well-mixed water column containing numerous eddies. The intensity of these eddies is greatest during June to October corresponding to the period of minimum inflow. Through the summer and early winter less saline water is advected from the east, stratifying the water column. The M_2 R_+ tidal current profile acts as a proxy measure of summer stratification. In addition, it highlights the decoupling of water column below the ice shelf draft from that above, allowing HSSW easier passage into the sub-ice shelf cavity. Consequently, the maximum inflow takes place during the period of maximum M_2 R_+ tides between December and April.

References

- Chapman, D.C., Dense water formation beneath a time-dependent coastal polynya, *J. Phys. Oceanogr.*, 29 (4), 807-820, 1999.
- Foldvik, A., T. Gammelsrød, E. Nygaard, and S. Østerhus, Current meter measurements near Ronne Ice Shelf, Weddell Sea: Implications for circulation and melting underneath the Filchner-Ronne ice shelves, *J. Geophys. Res.*, 2001.
- Gerdes, R., J. Determann, and K. Grosfeld, Ocean circulation beneath Filchner-Ronne Ice Shelf from three-dimensional model results, *J. Geophys. Res.*, 104 (C7), 15827-15842, 1999.
- Jenkins, A., D.M. Holland, K.W. Nicholls, M. Schröder, Seasonal ventilation of the cavity beneath Filchner-Ronne Ice Shelf simulated with an isopynic coordinate model, *J. Geophys. Res.*, Submitted.
- Makinson, K., Modeling tidal current profiles and vertical mixing beneath Filchner-Ronne Ice Shelf, Antarctica, *J. Phys. Oceanogr.*, 32 (1), 202-215, 2002.
- Makinson, K., and K.W. Nicholls, Modeling tidal currents beneath Filchner-Ronne Ice Shelf and on the adjacent continental shelf: their effect on mixing and transport, *J. Geophys. Res.*, 104 (C6), 13449-13465, 1999.
- Nicholls, K.W., and K. Makinson, Ocean circulation beneath the western Ronne Ice Shelf, as derived from in situ measurements of water currents and properties, in *Ocean, Ice, and Atmosphere: Interactions at the Antarctic Continental Margin*, edited by S.S. Jacobs, and R.F. Weiss, pp. 301-318, A.G.U., Washington DC, 1998.
- Nicholls, K.W., S. Østerhus, K. Makinson, and M.R. Johnson, Oceanographic conditions south of Berkner Island, beneath Filchner-Ronne Ice Shelf, Antarctica, *J. Geophys. Res.*, 106 (C6), 11481-11492, 2001.
- Nicholls, K.W., L. Padman, M. Schröder, R.A. Woodgate, A. Jenkins, and S. Østerhus, Water mass modification over the continental shelf north of Ronne Ice Shelf, Antarctica, *J. Geophys. Res.*, 108 (C8), 10.1029/2002JC001713, 2003.
- Renfrew, I.A., J.C. King, and T. Markus, Coastal polynyas in the southern Weddell Sea: Variability of the surface energy budget, *J. Geophys. Res.*, 107 (C6), 10.1029/2002JC000720, 2002.